Research Article

Nasir Ahmad, Khalid Khan, Sher Wali Khan, Haroon Ur Rashid*, Irum, Muhammad Zahoor*, Muhammad Naveed Umar, Riaz Ullah, Essam A. Ali

Homology modeling and molecular docking study of corticotrophin-releasing hormone: An approach to treat stress-related diseases

https://doi.org/10.1515/chem-2024-0069
received February 22, 2024; accepted June 30, 2024

Abstract: Corticotropin-releasing hormone receptors (CRHRs), also termed corticotropin-releasing factor receptors, are linked to G-protein-coupled receptor class. Corticotropin-releasing hormone (CRH) is medically significant in stress, immune response, gastrointestinal motility, and eating patterns. It serves as a releasing hormone and is encoded by the CRH gene. It has been established that there are two subtypes of CRHRs: CRH1-R and CRH2-R. These receptors, representing types 1 and 2, respectively, play a crucial role in regulating biological functions triggered by CRH. To treat stress-related gut abnormalities and stress-related disorders, regulation and optimization of CRH1-R and CRH2-R have turned into a novel idea. The three-dimensional (3D) structure of CRH is not completely recognized, and it is believed that the peptide key unit is helical and both the ultimate edges are relatively unsaturated. We can envisage its 3D structure from the amino acid order of a model protein by homology modeling procedures using Molecular Operating Environment and the Iterative Threading Assembly Refinement program. The assessment and authentication of the 3D structure were performed with RAMPAGE and ERRATE online servers. Utilizing the 3D structure of the target protein and predictions of its active site assists us in the development of new drug candidates aimed at treating disorders associated with stress. CRHR was docked with 19 CP376395 analogs acting as antagonists.

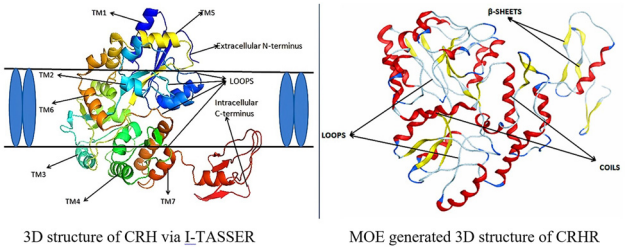

Graphical abstract

Keywords: homology modeling, molecular docking, corticotrophin, adenylate cyclase, nucleotides

1 Introduction

G-protein-coupled receptors (GPCRs) facilitate most of our biological feedback to neurotransmitters, hormones, and environmental stimulants, and so they possess a significant potential to act as therapeutic targets for a variety of diseases. [1]. The structure of GPCRs is usually comprised of seven α-helical transmembrane (TM) domains, an intracellular C-terminus, and an extracellular N-terminus [2,3]. Hydrophobic seven TM helical central core domain is linked by three intracellular and three extracellular loops. In extracellular loops 1 and 2, two cysteine residues are conserved to form a disulfide bridge, which is important for the stabilization and packing of a restricted number of conformations of seven TMs [4,5]. They are included in the cell membranes of a wide range of organisms including invertebrates, microorganisms, plants, and mammals [6,7]. All types of GPCRs share a common membrane topology, the

* **Corresponding author: Haroon Ur Rashid**, Center of Chemical, Pharmaceutical and Food Sciences, Federal University of Pelotas, Pelotas, 96010-900, RS, Brazil, e-mail: haroongold@gmail.com
* **Corresponding author: Muhammad Zahoor**, Department of Biochemistry, University of Malakand, Chakdara Dir Lower, 18800, Khyber Pakhtunkhwa, Pakistan, e-mail: mohammadzahoorus@yahoo.com
Nasir Ahmad, **Khalid Khan:** Department of Chemistry, Islamia College University, Peshawar, 25120, Khyber Pakhtunkhwa, Pakistan
Sher Wali Khan: Department of Chemistry, Rawalpindi Women University, 6th Road Satellite Town, Rawalpindi, 46300, Punjab, Pakistan
Irum: Center of Chemical, Pharmaceutical and Food Sciences, Federal University of Pelotas, Pelotas, 96010-900, RS, Brazil
Muhammad Naveed Umar: Department of Chemistry, University of Liverpool, Liverpool, United Kingdom
Riaz Ullah: Department of Pharmacognosy, College of Pharmacy, King Saud University, Riyadh, 11451, Saudi Arabia
Essam A. Ali: Department of Pharmaceutical Chemistry, College of Pharmacy, King Saud University, Riyadh, Saudi Arabia

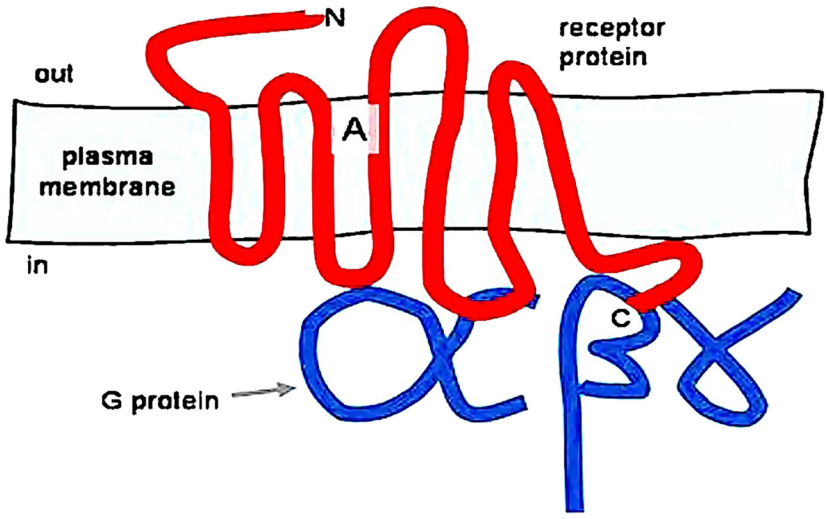

Figure 1: GPCR in the plasma membrane with seven α-helical TM sections. Heterotrimeric G-protein is characterized diagrammatically by the letters α, β, and γ in the cytoplasm. Diagram showing label A, an agonist in its binding pocket; C, receptor C-terminus in the cytoplasm; and N, receptor extracellular N-terminus. [Ref. 6] The figure is recorded under the Creative Commons Attribution 4.0 International Agreement, which approves unconditional practice, distribution, amendment, and replication in any means, http://creativecommons.org/licenses/by/4.0/.

N-terminus is outside, and the C-terminus is inside with seven alpha-helical TM segments (Figure 1) [8,9].

GPCRs represent the largest group of plasma membrane receptors. Rhodopsin and adrenergic receptors are the most common types of GPCRs.

GPCRs are the receptors for a large amount of different signals. The most important among them are the chemosensory GPCRs, which act as receptors for the external origin that are odors, pheromones, or tastes. Mainly other GPCRs react to endogenous signals such as peptides, lipids, neurotransmitters, or nucleotides [4]. They represent essential plasma membrane proteins that transmit signals from extracellular ligands in intracellular relay proteins, the heterotrimeric GTP-binding proteins (G proteins). The G proteins initiate pleiotropic modifications in numerous targets by coupling to several downstream effectors. Thus, the extracellular signal is characteristically intensified to create vigorous, wide-ranging, and cell-specific responses [10]. GPCRs can be triggered by various exterior stimuli, including peptides, chemoattractants, hormones, neurotransmitters, phospholipids, odorants, photons, and taste ligands [11–13]. GPCRs are activated through ligands and are signaled through G proteins that are made of α, β, and γ subunits. The α- and β/γ-subunits disintegrate and discretely trigger several conventional effectors such as phospholipases and adenylyl cyclases. They also modulate the action of several kinases, ion transporters, and ion channels.

GPCRs are classified into five families. Its classification is based on the similarity of amino acid sequences within the seven TM helical segments.

Class A, the rhodopsin family, consists of 701 members.

Class B1, the secretin family, consists of 15 members.

Class B2, the adhesion family, consists of 24 members.

Class C, the glutamate family, consists of 15 members.

Class F, the frizzled/taste 2 family, consists of 24 members [14,15].

Corticotropin-releasing hormone (CRH) targets a membrane-bound GPCR and acts as a primary hormone in the flight or fight responses. It is a 41-amino acid polypeptide made from 196 amino acids, a precursor of CRH by C-terminal cleavage. The peptide of CRH can be segmented into three useful parts. The residues (1–16) are believed to be vital for receptor activation and agonist binding. The residues (17–31) containing the CRH-binding protein (CRHBP) control the structural conformation of the protein, while the residues (32–41) are essential for receptor binding [16,17]. CRH has been recognized and identified in mammals, amphibians, fishes, and birds [18].

CRH is made in smaller quantities by certain white blood cells, and it causes swelling particularly that of the gut. Moreover, it is also secreted by the paraventricular nucleus of the hypothalamus [19]. CRH is principally produced in the hypothalamus. Additionally, it is also discharged into the hypophyseal portal passage in response to stress [20].

CRH is accountable for autonomic, endocrine, behavioral, and immunological responses to stress in mammals [21]. The key central regulator of the hypothalamic–pituitary–adrenal (HPA) axis is CRH, which regulates the HPA through the initiation of the proopiomelanocortin gene

and the discharge of corticotropin adrenocorticotropic hormone from the anterior pituitary [22,23]. Stress has a suppressive effect on the male and female reproductive systems; the stress system is triggered in a synchronized way, which influences the chief and peripheral roles that are vital for survival and adaptation during stress [24]. In humans and other mammals, two receptor genes have been identified to date. Both receptors of CRH consist of seven TM regions that are coupled to adenylate cyclase. CRH and its receptors are present in a variety of tissues including the immune system, blood–brain barrier, gastrointestinal tract, and parasympathetic ganglion [20]. The distribution of both receptors in various tissues is different. CRH-R1 is present all over the brain and is greatly expressed in the anterior pituitary [24]. Corticotropin-releasing hormone receptor 2 (CRHR2) is dispersed in the wider regions of the human brain. Its subtype CRH-R2a is exclusively present in the brain and has a wider distribution than the CRH-R1. CRH-R2b is highly expressed in skeletal muscles and the heart. The expression of CRH-R2a and CRH-R2b in different regions suggests their different functional roles [17,22,25]. CRH and its receptors are found in the male and female reproductive system in addition to their presence in the different extrahypothalamic sites of the central nervous system [24].

CRHBP is considered to act as a secreted protein that modulates the actions of CRH. The CRHBPs are synthesized in the liver in addition to their expression in the human brain. They have a significant impact on the availability of CRH. [22]. The CRH, its binding protein, and both receptors are crucial for regulating the HPA axis. Women have a higher level of plasma CRHBPs than men. CRHBP contains ten cysteine residues, and its secondary structure consists of five loops [26].

The three-dimensional (3D) structure of CRH is not established. In an ideal situation, we can predict the protein structure accurately. With the help of computer software as experimental tools, we perform homology modeling. A 3D model of the protein is needed, which can be constructed using the homology modeling technique, as neither X-ray crystallography nor NMR spectroscopy is capable of determining such a model [10,27]. The models built through homology modeling provide a great deal of information about how the protein functions. A suitably designed model will closely resemble unknown proteins. The quality of the model is evaluated, and the best model is selected among the obtained models. The model quality is directly proportional to the similarity with the target and template protein. The quality of the model decreases with the decrease in the similarity of the target and model. Protein Data Bank (PDB) provides the foundation of homology modeling via known 3D structures (templates) available in it.

Our study aims to predict a potential 3D model of CRH via homology modeling and molecular docking techniques for the discovery of novel drug molecules to treat stress-related conditions. It is important to mention that the current study is theoretical and speculative. Consequently, experimental investigations would be necessary in the future to endorse the results obtained in this *in silico* work.

2 Methodology

2.1 Protein sequence retrieval

The primary sequences of CRH with accession no G3CIS4 were received from Universal Protein Resources (UniProt) [28] in FASTA format (Fast protein or nucleotide comparison). Its 3D structure was unavailable and was therefore designed via homology modeling employing Iterative Threading Assembly Refinement (I-TASSER) [29,30] and Molecular Operating Environment (MOE) [31].

2.2 Homology model prediction by GPCR I-TASSER server

GPCR I-TASSER method [29] is a hybrid method for the estimation of the 3D structure of GPCRs. The I-TASSER server includes the following major steps:

(a) The amino acid arrangement of a single protein is copied and pasted, an optional name is given to the protein, and the job is run.
(b) I-TASSER applies a Local Meta-Threading Server, version 3 (LOMETS) [32] with additional threading programs, i.e., FUGUE [33], HHSEARCH [34], MUSTER [35], PROSPECT [36], PPA [37], SP^3 [38], and SPARKS [39]. Using the *Z*-score, the top template alignments were selected for further consideration. The standard of the template arrangement is determined through the *Z*-score.
(c) In template structures, fragments were excised from the threading alignments, and structure assembly was performed.
(d) Model selection and refinement occurred on the I-TASSER second run. Subsequently, structure-based functional annotation is performed.

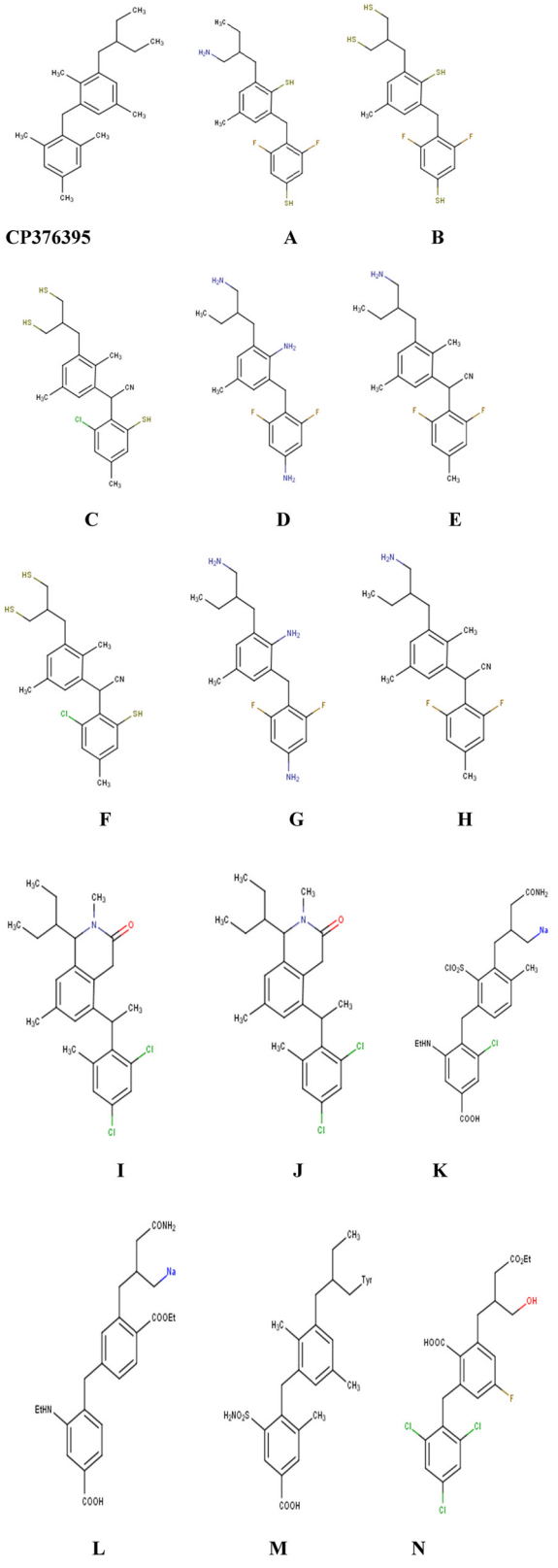

Figure 2: Chemical structures of CP376395 and its derivatives.

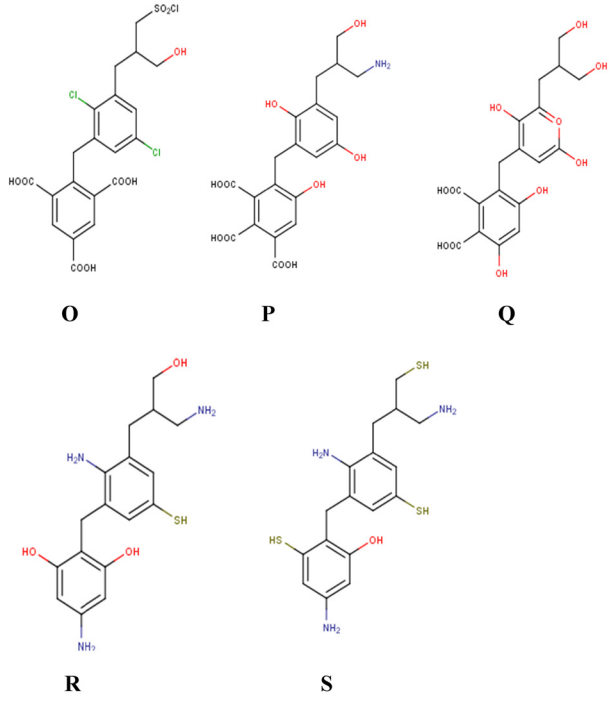

Figure 2: (*Continued*)

When the job run was completed, the I-TASSER result page was available in the inbox (via email).

2.3 Homology model construction through MOE

A 3D model of CRH was made through MOE. To produce the precise 3D design of CRH, key steps, i.e., recovery of the pattern, sequence arrangement, generation of the design, justification, and refinement, were followed. Before the aforementioned steps for model generation, parameters such as the force field Amber 99 and model scoring to GB/VI (Generalized Born/Volume Integral) were adjusted. After the sequence alignment, root mean square deviation (RMSD) values for αC atoms, side row atoms, and backbone atoms, and each arrangement of all heavy atoms were calculated. The most stable structure was recognized after the method that was then recovered in PDB layout.

2.4 Molecular docking

Molecular docking is a computational technique through which the most appropriate orientation between two

```
>G000574
MGGHPQLRLVKALLLLGLNPVSASLQDQHCESLSLASNISGLQCNASVDLIGTCWPRSPA
GQLVVRPCPAFFYGVRYNTTNNGYRECLANGSWAARVNYSECQEILNEEKKSKVHYHVAV
IINYLGHCISLVALLVAFVLFLRLRSIRCLRNDQADGALEVGAPWSGAPFQVRRSIRCLR
NIIHWNLISAFILRNATWFVVQLTMSPEVHQSNVGWCRLVTAAYNYFHVTNFFWMFGEGC
YLHTAIVLTYSTDRLRKWMFICIGWGVPFPIIVAWAIGKLYYDNEKCWFGKRPGVYTDYI
YQGPMILVLLINFIFLFNIVRILMTKLRASTTSETIQYRKAVKATLVLLPLLGITYMLFF
VNPGEDEVSRVVFIYFNSFLESFQGVRSAIRKRWHRWQDKHSIRARVARAMSIPTSPTRVS
FHSIKQSTAV
```

Figure 3: Query sequence of G3CIS4 having 430 residues.

molecules is predicted. The technique is used to predict protein binding sites, pockets, and clefts of the ligands [40,41]. The 3D framework of CRHR was made by homology modeling for molecular docking. The 3D protonation and energy minimization of the receptor molecule was performed via force field Amber 99. For the molecular docking of CP376395 derivatives, the default domain of the MOE-dock database was used. At the end of docking, the binding interactions of all derivatives (Figure 2) with homology-modeled CRHR were predicted.

2.5 Primary sequence retrieval

The principal arrangement of CRH with accession no G3CIS4 in FASTA format was taken from UniProt containing 430 amino acid sequences (Figure 3).

2.6 Homology model prediction by GPCR I-TASSER server

The 3D framework of CRH was built with the online server GPCR I-TASSER. In total, five patterns were predicted, and the TM-score, *C*-score, and RMSD values for the first design are given. The *C*-score is an approximation of the grade of the projected model. The *C*-score value generally falls within the range of [−5, 2], where a higher score indicates a model of superior quality. In the top five patterns, the first one with a greater *C*-score of −0.45 was downloaded in PDB format. TM score shows the constitutional resemblance between the projected model and the original structure. TM score value typically ranges in [0, 1]. The predicted TM score and RMSD values for the initial design are 0.66 ± 0.13 and 8.0 ± 4.4 Å, respectively (Table 1). These values are acceptable for further studies. The 3D structure of CRH (first ranked model) contains seven TM helices (7TM), intracellular C-terminal G-protein-coupled site, CRH-binding site extracellular N-terminus, and extra and intracellular loops (Figure 4).

Table 1: Statistical analysis of a 3D model of CRH

C-score	Predicted TM score	Predicted RMSD score
−0.45	0.66 ± 0.13	8.0 ± 4.4 Å

2.7 Homology modeling construction through MOE

MOE 2011-12 package was employed for the generation of the design. At the end of the process, ten models were generated and the most stable ones were selected and recovered in the PDB form. The native model was overlaid on the template to generate a superimposed model. A close homology was confirmed by an RMSD value of 1.24 Å (Figure 5).

2.8 Justification and assessment of the final model

To justify the quality and accuracy of the final model, several steps were performed during the analysis of the final 3D model.

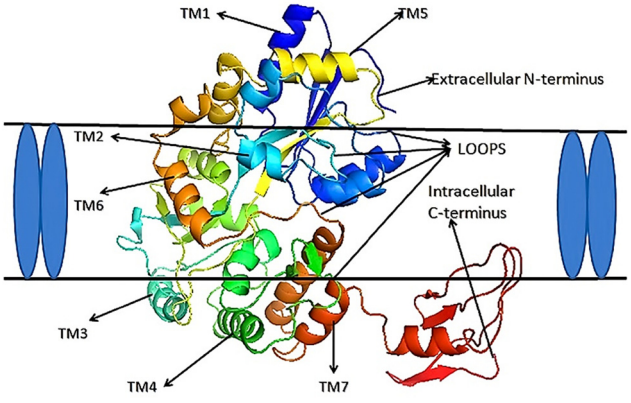

Figure 4: 3D structure of CRH via I-TASSER.

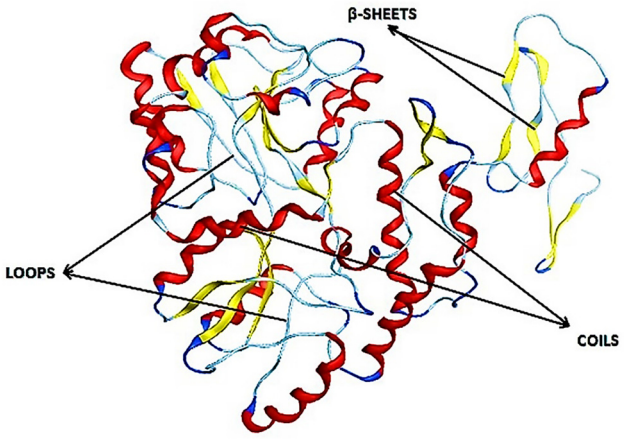

Figure 5: MOE generated 3D structure of CRHR.

For the stereochemical quality analysis, a Ramachandran plot was obtained. Ramachandran plot was obtained using the RAMPAGE server [42,43]. The results (Figure 6) were obtained to give the relation between the torsional angle with the Ramachandran plot and protein structure. Psi angle is between the carboxylic group and α-carbon. The results show that 91.1%, 6.8%, and 2.1% of the residues fell within the favored, allowed, and disallowed zones of the Ramachandran plot, respectively (Table 2). Almost 98% of the residues have fallen in the most favored and allowed regions. Through MOE2011-12 software, the Ramachandran plot analysis also showed that the residues PRO-6, ILE-300, TRP 55, ARG-66, SER-58, ALA-168, PHE-269, PRO-164, and GLN-62 were out of the dynamically favored zones. The residues remaining in the central zones of the Ramachandran plot indicate the high consistency of the last structure.

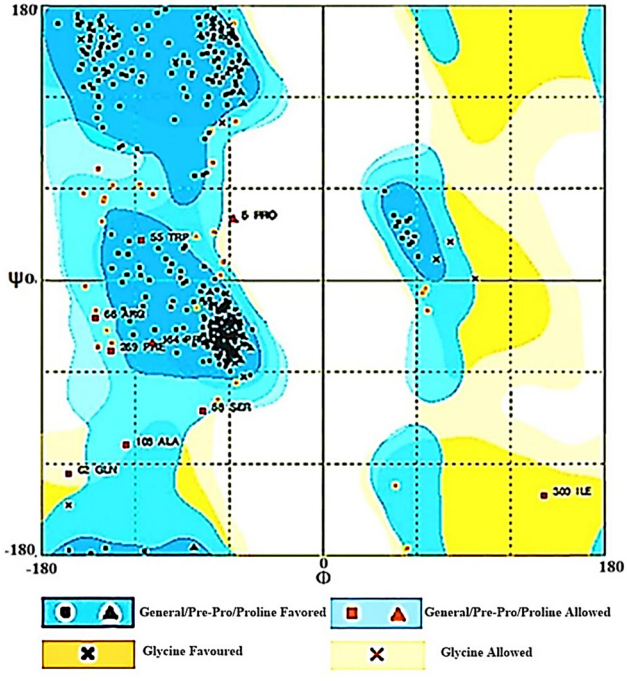

Figure 6: Ramachandran plot shows the results of CRH. Rampage results showed 91.1% favored, 6.8% allowed, and 2.1% disallowed. PRO-6, ILE-300, ALA-168, GLN-62, SER-58, PHE-269, TRP-59, ARG-66, and PRO-164 were out of the energetically favorable region.

The total caliber of the final design was predicted through the ERRATE server [44,45]. An ERRATE score of 82.816 was obtained. This value shows that it is a high-quality model as a 50 score is considered good. ERRATE is generally applied to explain the non-bonded interactions between various atoms. The gray bar indicates the zone of error, the black bar shows the misfolded zone, and the white bars reveal the zone for the folding of a protein possessing less error rate (Figure 7a and b).

2.9 Molecular docking of CRH with CP376395 derivatives

According to the molecular docking results, derivative **A** exhibited a maximum of two interactions with a docking score of −15.74 kcal/mol within the enzyme's binding pocket. A total of seven amino acid fragments are situated in the binding pocket of the receptor, whereas the Lys 11 residue lies in TM domain 1 (TM1) and forms two interactions. Lys11 residue shows a hydrogen bonding interaction and an arene–cationic interaction with the electrophile NH_2 of cyclobutane and the SH group of the benzene ring, respectively. The RMSD value was noted to be 3.734 Å.

Only one interaction is shown by derivative **B**. A total of four amino acid fragments are located in the binding pocket of the receptor, and an arene–arene interaction is shown by Tyr 281 (lying in the TM5) with the benzene ring. The docking score and RMSD value were noted to be −11.57 Kcal/mol and 1.662 Å, respectively.

Two interactions are shown by the derivative **C**. A total of four amino acid fragments are situated in the binding pocket of the receptor. The residues Arg 403 and Arg 174 lie in the TM7 and TM4, respectively. Both the residues show arene–arene interactions with the benzene ring. The docking score and RMSD value were noted to be −14.88 Kcal/mol and 4.102 Å, respectively.

Table 2: Plot statistics of the modeled CRHRs

Plot investigation		
Residues fell in the favored region (98.0%) projected	(390)	91.1%
Residue fell in the allowed region (2%) projected	(29)	0.68%
Residue fell in the disallowed region	(9)	2.1%

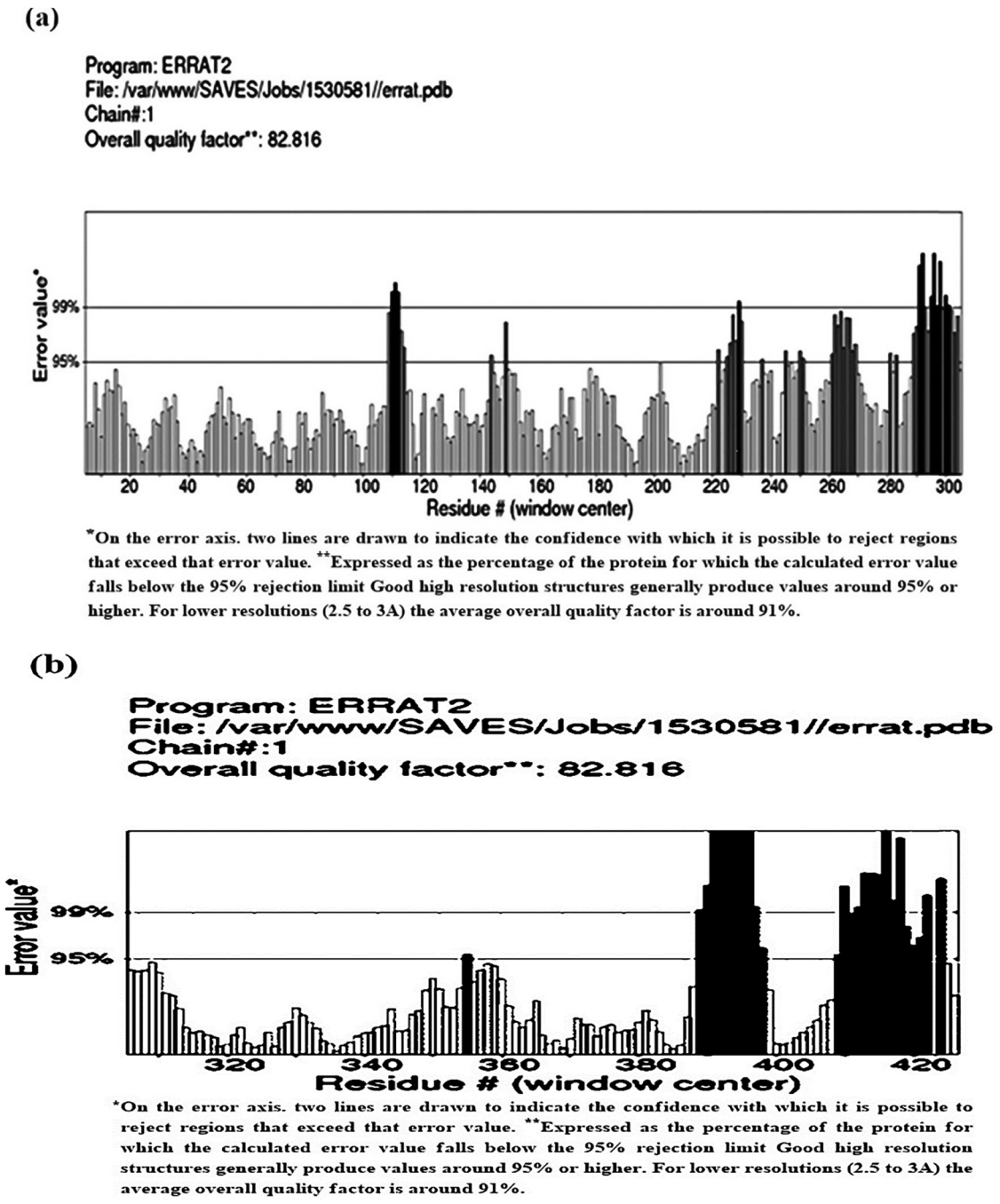

Figure 7: (a) and (b) An overall quality factor of CRH predicted by ERRAT 2.

A maximum of two interactions are shown by derivative **D**. A total of four amino acids are situated in the binding pocket of the receptor. The residues Arg 392 and Arg 395 are located in TM6, and both establish arene–cationic bonds with the same benzene skeleton. The docking score and RMSD value were recorded to be −15.60 kcal/mol and 2.126 Å, respectively.

A maximum of three interactions are shown by derivative **E**. A total of four amino acids are situated in the binding pocket of the receptor. The residues Arg 403 and Arg 174 are located in TM7 and TM4, respectively. Two arene–cationic interactions are established by Arg 403 with a benzene ring. On the other hand, the residue Arg 174 forms an arene–cationic bonding with another benzene skeleton. The docking score and RMSD value were noted to be −14.25 kcal/mol and 3.624 Å, respectively.

A maximum of two interactions are formed by derivative **F**. A total of four amino acids are situated in the

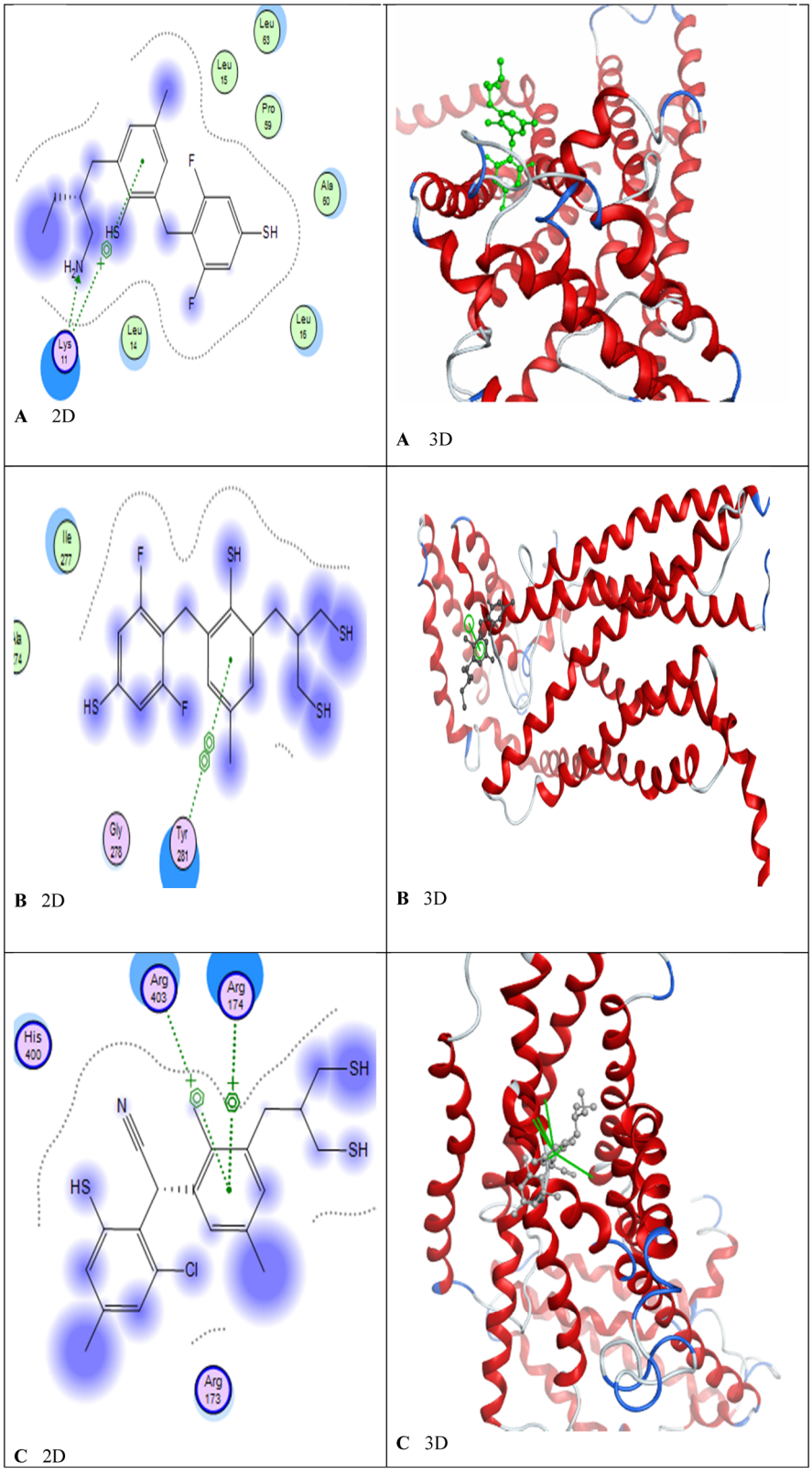

Figure 8: 2D and 3D interaction images of CRH with CP376395 derivatives **(A–J)**.

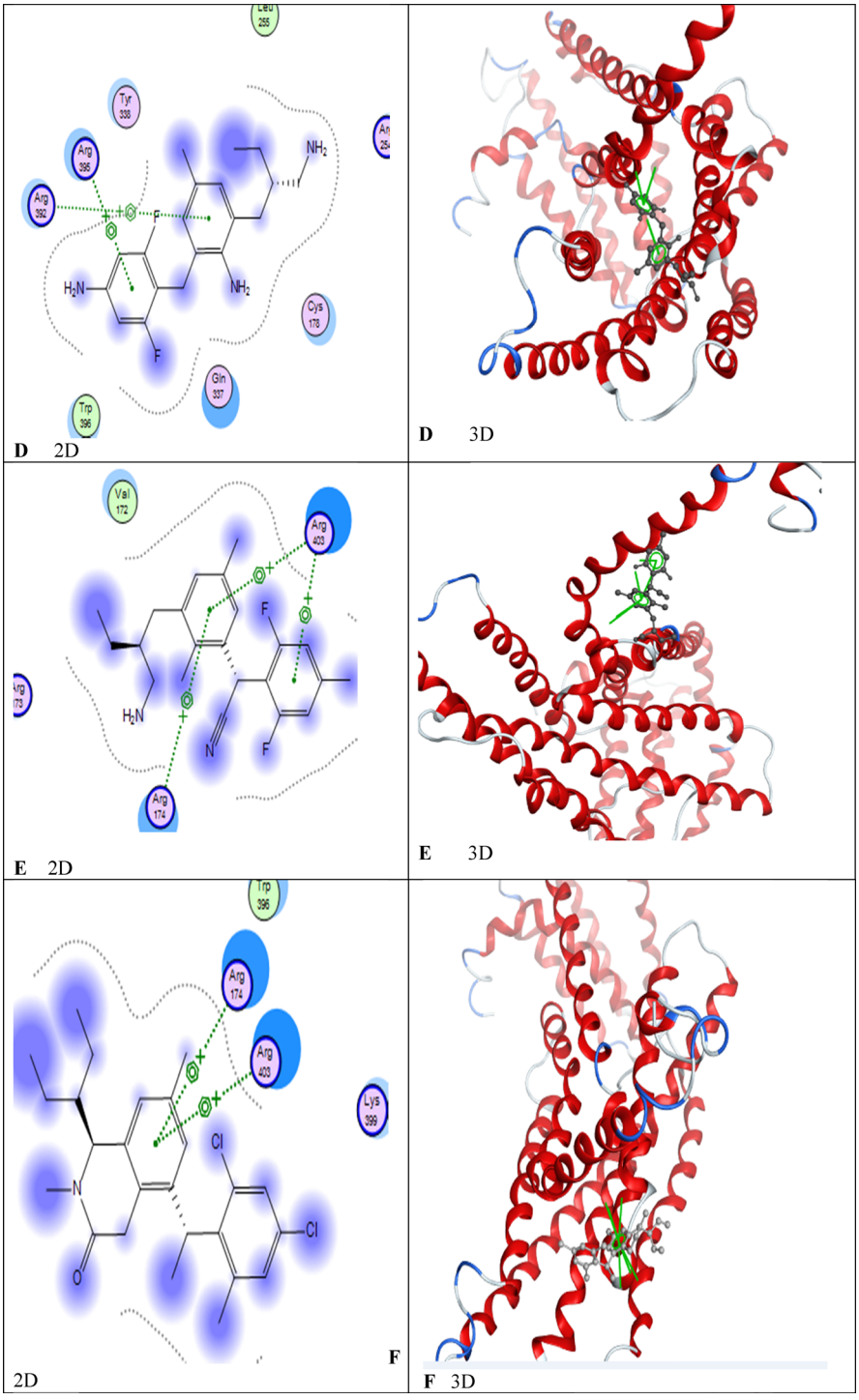

Figure 8: (*Continued*)

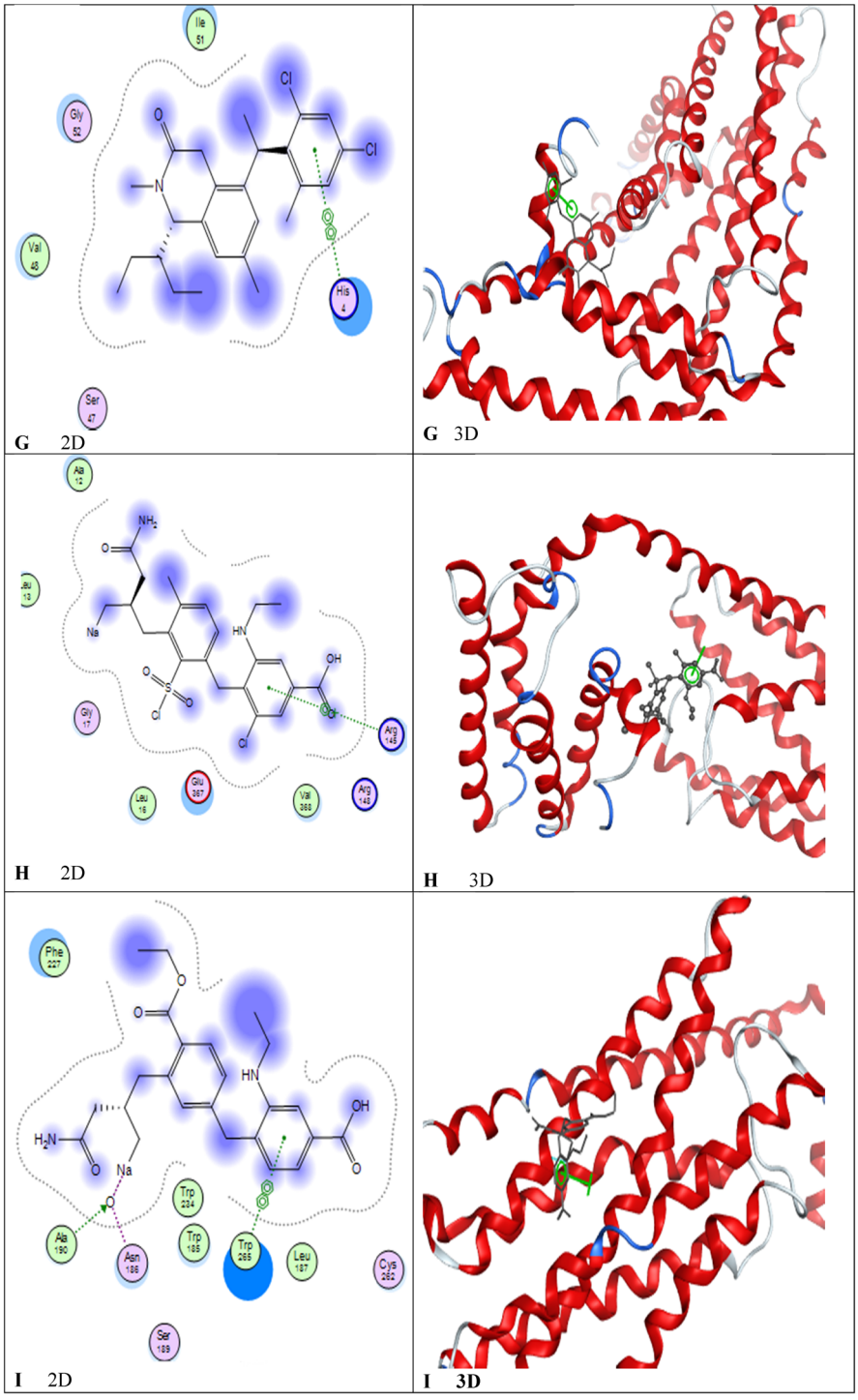

Figure 8: (*Continued*)

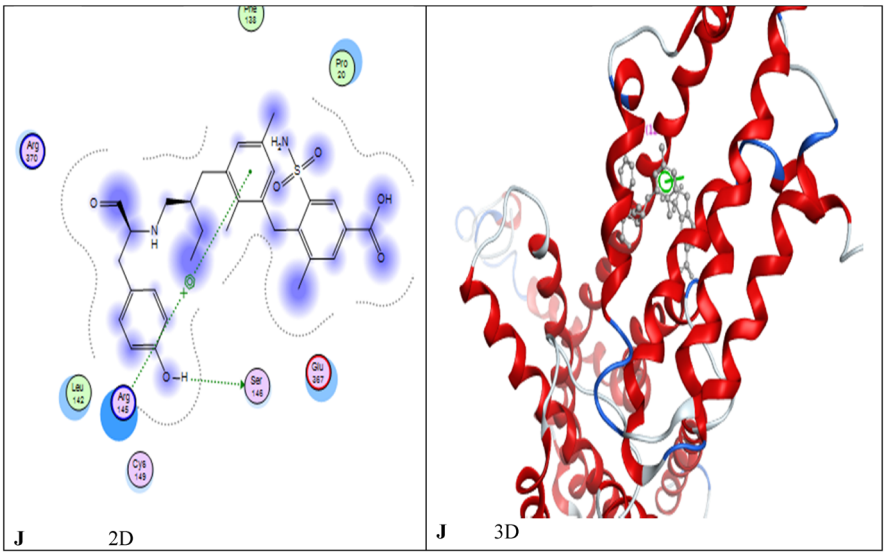

Figure 8: (*Continued*)

binding pocket of the receptor. The residues Arg 403 and Arg 174 are located in TM7 and TM4, respectively. Both the residues form arene–cationic bondings with the same benzene skeleton. The docking score and RMSD value were recorded to be 20.06 kcal/mol and 4.353 Å, respectively.

Only one interaction is shown by derivative **G**. A total of five amino acids are situated in the binding pocket of the receptor. The residue His 4 is located at the N-terminal and forms an arene–arene bonding with the benzene skeleton. The docking score and RMSD value were recorded to be −19.41 kcal/mol and 2.246 Å, respectively.

Only one interaction is shown by derivative **H**. A total of eight amino acids are situated in the binding pocket of the receptor. The residue Arg 145 is situated in TM3 and forms an arene–cationic bonding with the benzene skeleton. The docking score and RMSD value were verified to be −16.42 kcal/mol and 3.443 Å, respectively.

A maximum of three interactions are shown by derivative **I**. A total of nine amino acids are situated in the binding pocket of the receptor. The residue Trp 266 is located in TM5, and the two residues (Ala 190 and Asn 186) are situated in TM4. An arene–arene interaction is noted between the residue Trp 266 and the benzene moiety. The residues Ala 190 and Asn 186 form hydrogen bonding separately with the same oxygen. The docking score and RMSD value were confirmed to be −18.57 kcal/mol and 2.824 Å, respectively.

Two interactions are formed by derivative **J**. A total of eight amino acids are situated in the binding pocket of the receptor. The residue Arg 145 (located in TM3) forms an arene–cationic bonding with the benzene moiety, and the residue Ser 146 (located in TM3) establishes a hydrogen bonding with the hydroxyl moiety connected to a benzene ring. The docking score and RMSD value were noted to be −15.60 kcal/mol and 2.126 Å 2.824 Å, respectively.

The overall docking results of the CRH with CP376395 derivatives **(A–J)** are provided in Figure 8 and Table 3.

Only one interaction is established by derivative **K**. A total of seven amino acids are situated in the binding pocket of the receptor. The residue Thr 417 is located at the C-terminal and establishes a hydrogen bonding with the hydroxyl moiety of the ligand. The docking score and RMSD value were noted to be −16.02 kcal/mol and 1.857 Å, respectively.

A maximum of three interactions are shown by derivative **L**. A total of eight amino acids are situated in the binding pocket of the receptor. The residue Ser 24 is located in TM1, and the two residues (Arg 292 and Lys 286) are situated in TM5. A hydrogen bonding is observed

Table 3: Docking results of CP376395 derivatives **(A–J)**

CP376395 analogs	Docking score (kcal/mol)	RMSD (Å)	Number of interactions
A	−15.74	03.734	02
B	−11.57	01.662	01
C	−14.88	04.102	02
D	−15.60	02.126	02
E	−14.25	03.624	03
F	−20.06	04.353	02
G	−19.41	02.246	01
H	−16.42	03.443	01
I	−18.57	02.824	03
J	−15.60	02.126	02

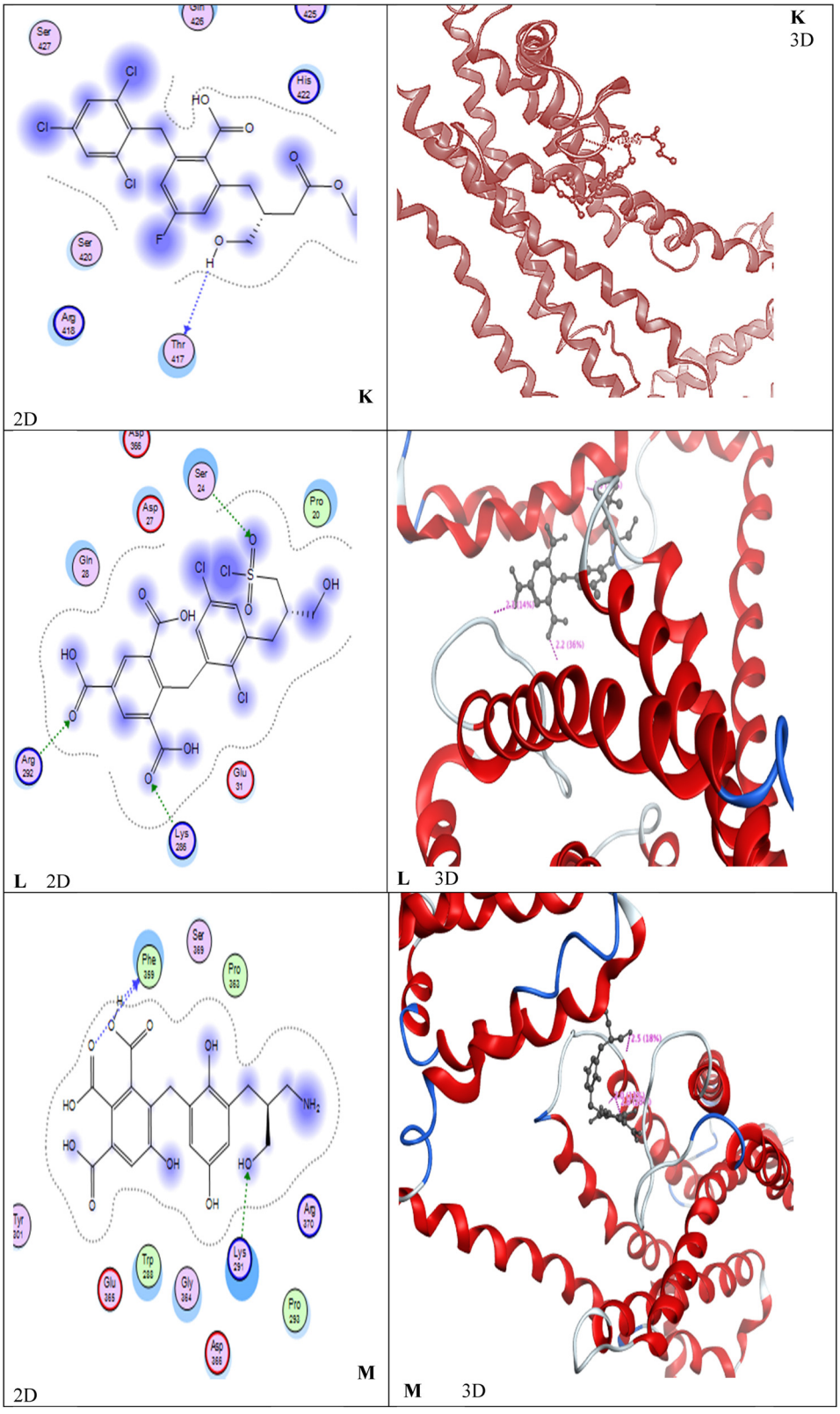

Figure 9: 2D and 3D interaction images of CRH with CP376395 derivatives **(K–S)**.

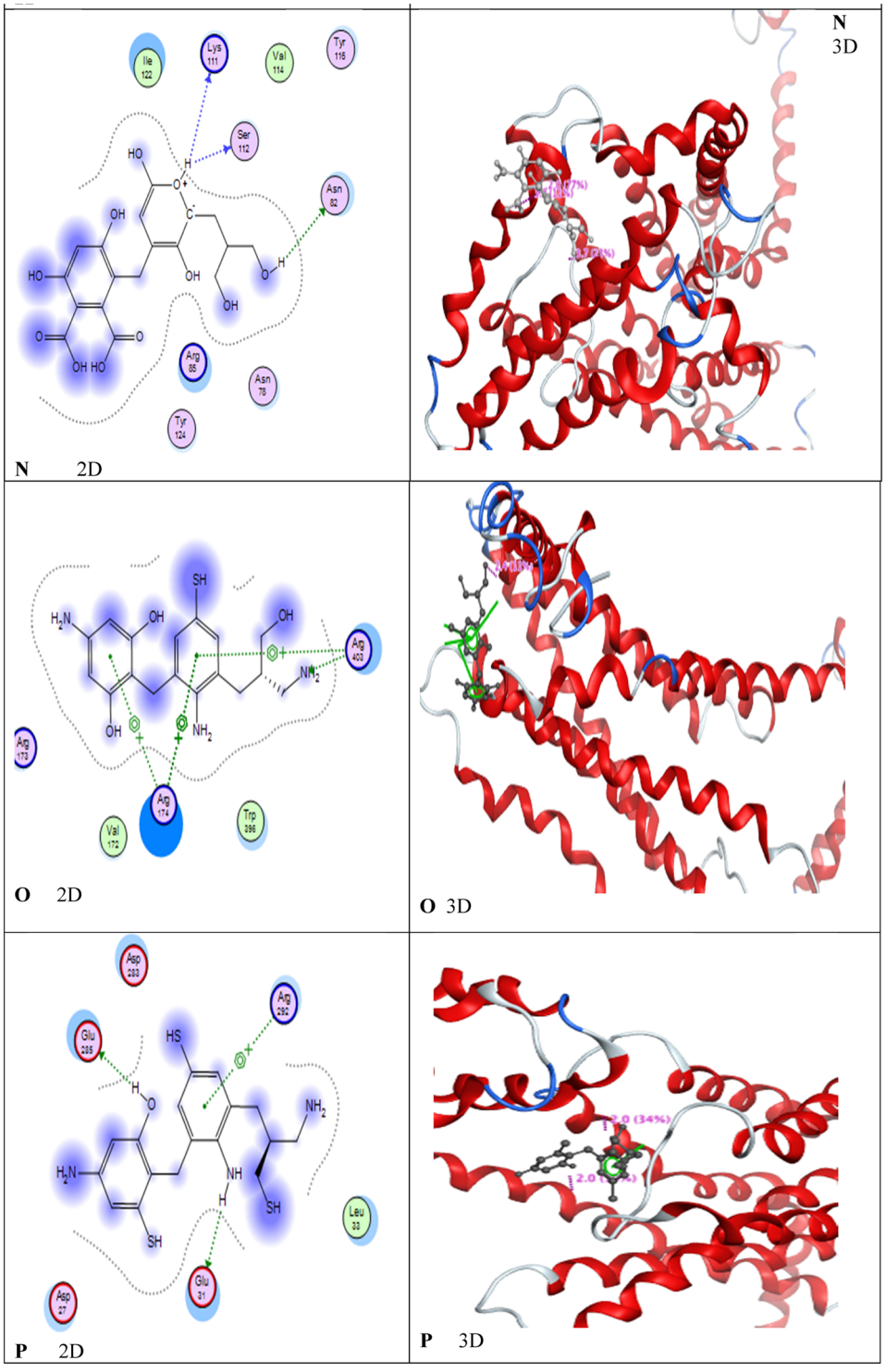

Figure 9: (*Continued*)

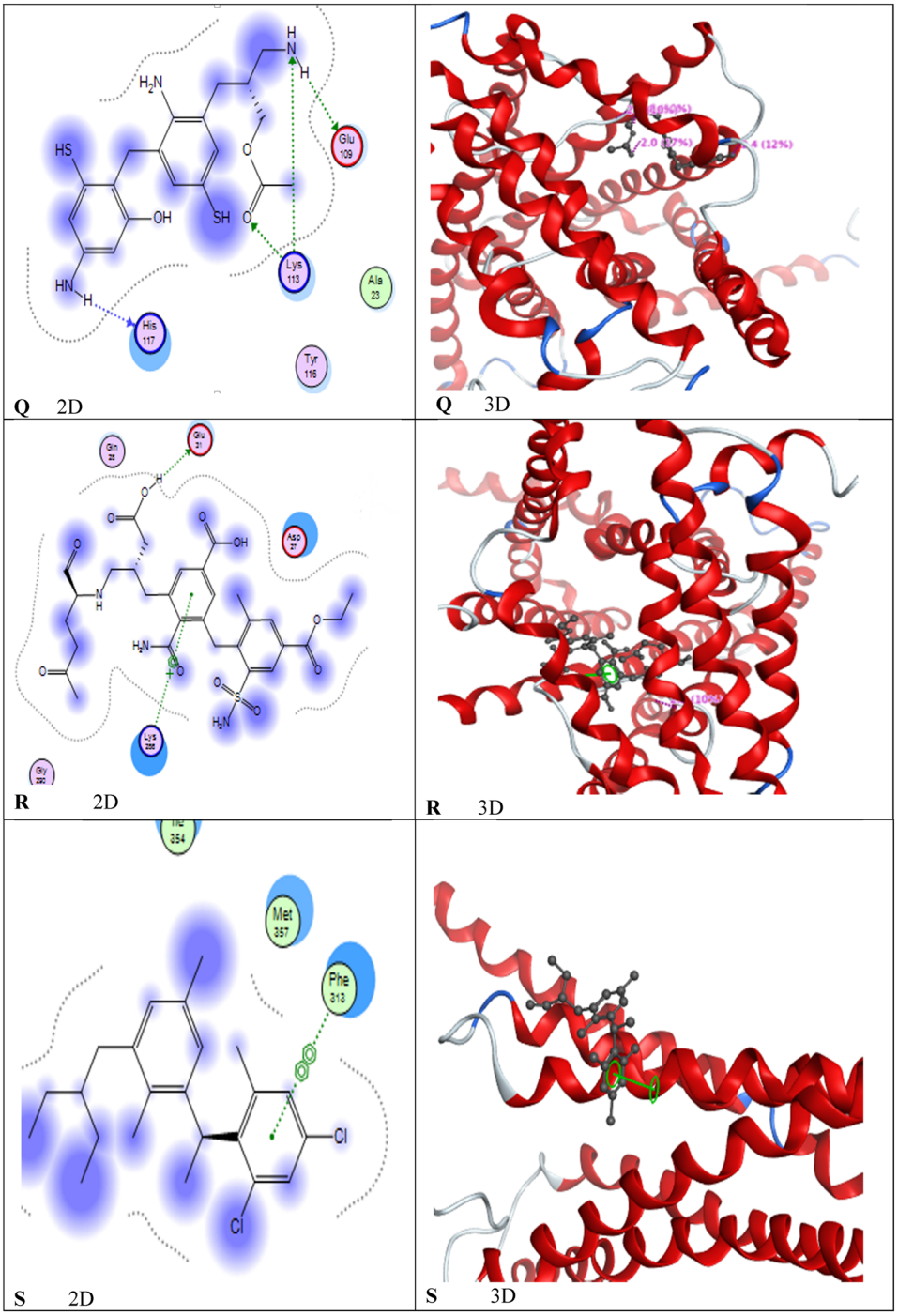

Figure 9: (*Continued*)

between the residue Ser 24 and the oxygen of the SO_2Cl moiety. A second hydrogen bonding is found between the residue Arg 292 and the oxygen of the carboxylic moiety. The third hydrogen bonding is formed between the residue Lys 286 and the oxygen of another carboxylic moiety. The docking score and RMSD value were noted to be −15.57 kcal/mol and 3.331 Å, respectively.

A maximum of three interactions are shown by derivative **M**. A total of 11 amino acids are found in the binding pocket of the receptor. The residues Lys 291 and Phe 359 are located in TM5 and TM6, respectively. The residue Lys 291 forms a hydrogen bond with the hydroxyl group of the ligand. The residue Phe 359 forms two hydrogen bonds with the oxygen of the carboxylic moiety and the hydrogen

Table 4: Docking results of CP376395 derivatives **(K–S)**

CP376395 analogs	Docking score (kcal/Mol)	RMSD (Å)	Number of interactions
K	−16.02	01.857	01
L	−15.57	03.331	03
M	−16.69	03.763	03
N	−25.27	03.639	03
O	−19.89	16.65	04
P	−17.51	01.554	03
Q	−16.92	03.385	04
R	−26.38	02.185	01
S	−16.09	01.287	01

of the hydroxyl moiety. The docking score and RMSD value were noted to be −16.69 kcal/mol and 3.763 Å, respectively.

A maximum of three interactions are shown by derivative **N**. A total of nine amino acids are situated in the binding pocket of the receptor. The residues Lys 111, Ser 112, and Asn 89 are all found in TM3. The residues Lys 111 and Ser 112 both make hydrogen bonds with hydrogen of the same hydroxyl moiety on the ligand molecule. On the other hand, the residue Asn 89 also forms a hydrogen bond with the hydrogen of a different hydroxyl moiety on the ligand molecule. The docking score and RMSD value were noted to be −25.27 kcal/mol and 3.639 Å, respectively.

A maximum of four interactions are shown by derivative **O**. A total of five amino acids are present in the binding pocket of the receptor. The residues Arg 174 and Arg 403 are located in TM4 and TM7, respectively. The residue Arg 174 forms two arene–cationic interactions with two different aromatic rings. On the other hand, the residue Arg 403 forms an arene–cationic interaction and a hydrogen-bonding interaction with an aromatic ring and the amino group of aniline moiety, respectively. The docking score and RMSD value were recorded to be −19.89 kcal/mol and 16.65 Å, respectively.

A maximum of three interactions are displayed by derivative **P**. A total of six amino acids are present in the binding pocket of the receptor. The residues Glu 31 is found in TM1, whereas the residues Arg 292 and Glu 285 are both situated in TM5. The residue Arg 292 forms an arene–cationic interaction with the aromatic moiety of the ligand molecule. On the other hand, the residues Glu 31 and Glu 285 both establish hydrogen bonds with the hydrogen of an amino moiety and the hydrogen of a hydroxyl group, respectively. The docking score and RMSD value were observed to be −17.54 kcal/mol and 1.554 Å, respectively.

A maximum of four interactions are shown by derivative **Q**. A total of five amino acids are present in the binding pocket of the receptor. Three residues Glu 109, His 117, and Lys 113 all are located in TM3. A hydrogen bond between the residue Glu 109 and the hydrogen of the amino moiety is observed. The residue Lys 113 forms two hydrogen-bonding interactions with the nitrogen of an amino moiety and the doubly bonded oxygen atom of the carboxylic moiety. The fourth hydrogen-bonding interaction is displayed between the residue His 117 and the hydrogen of the amino group. The docking score and RMSD value were identified to be −16.92 kcal/mol and 3.385 Å, respectively.

A maximum of two interactions are shown by derivative **R**. A total of five amino acids are found in the binding pocket of the receptor. The residues Glu 21 and Lys 256 are present in TM1 and TM5, respectively. A hydrogen bond is observed between the residue Glu 21 and the hydrogen of the carboxylic moiety. An arene–cationic interaction is formed between the residue Lys 256 and an aromatic ring of the ligand molecule. The docking score and RMSD value were identified to be −26.38 kcal/mol and 2.185 Å, respectively.

Only one interaction is shown by derivative **S**. A total of three amino acids are found in the binding pocket of the receptor. The residue Phe 313 is found in TM6, which forms an arene–arene interaction with an aromatic ring of the ligand molecule. The docking score and RMSD value were recognized to be −16.09 kcal/mol and 1.287 Å, respectively.

The overall docking results of CRH with CP376395 derivatives **(K–S)** are provided in Figure 9 and Table 4.

3 Conclusion

The key goal of this study is to design a 3D structure of CRH through computational work and to find the active sites for drug designing to affect their biological and biochemical activities. The 3D structure of CRHRs was architected by MOE and the I-TASSER package. The justification and assessment of the final model of CRHRs were made with RAMPAGE and ERRATE online servers. Molecular docking studies revealed that CRH exhibited robust interactions with the drug CP376395 and its analogs. It was noted that CP376395 derivatives O and Q showed a maximum of four interactions with CRH with a decent docking score. In contrast, the analogs E, I, L, M, N, and P each displayed a maximum of three interactions with CRH, accompanied by decent docking scores. The results showed good docking scores for most of the CP376395 derivatives after their molecular docking with the CRH. These investigations will support us to know the 3D structure of CRHRs and their function. Furthermore, the current study will propose a hypothetical path for chemists to design new drug candidates for the treatment of stress-related diseases.

Acknowledgment: The authors extend their appreciation to the researchers supporting Project Number RSP2024R45 King Saud University, Riyadh, Saudi Arabia.

Funding information: This study was supported by researchers supporting Project Number (RSP2024R45), King Saud University, Riyadh, Saudi Arabia.

Author contributions: N.A.: conceptualization, validation, software, and writing the original draft; K.K.: project administration, conceptualization, and visualization; S.W.K.: visualization, investigation, and software; H.ur.R.: software, validation, writing, review and editing; I.: formal analysis and investigation; M.Z.: data validation, visualization, and editing; R.U. and E.A.: funding acquisition and technical assistance. All authors read and approved the final manuscript.

Conflict of interest: All the authors declare hereby that they have no conflict of interest.

Ethical approval: The conducted research is not related to either human or animal use.

Data availability statement: All the data are presented in this manuscript. There are no associated data in any repository.

References

[1] Grossfield A. Recent progress in the study of G protein-coupled receptors with molecular dynamics computer simulations. Biochim Biophys Acta. 2011;1808(7):1868–78. doi: 10.1016/j.bbamem.2011.03.010.

[2] Yang D, Zhou Q, Labroska V, Qin S, Darbalaei S, Wu Y, et al. G protein-coupled receptors: Structure- and function-based drug discovery. Signal Transduct Target Ther. 2021;6(1):7. doi: 10.1038/s41392-020-00435-w.

[3] Peng ZL, Yang JY, Chen X. An improved classification of G-protein-coupled receptors using sequence-derived features. BMC Bioinf. 2010;11:420. doi: 10.1186/1471-2105-11-420.

[4] Cardoso JC, Clark MS, Viera FA, Bridge PD, Gilles A, Power DM. The secretin G-protein-coupled receptor family: teleost receptors. J Mol Endocrinol. 2005;34(3):753–65. doi: 10.1677/jme.1.01730.

[5] Ahmad N, Khan K, Rashid Ur H, Khan SW, Umar MN, Gulfam N, et al. Homology modeling and molecular docking study of metabotropic glutamate receptor 5 variant F: an attempt to develop drugs for treating CNS diseases. Z Phys Chem. 2024. doi: 10.1515/zpch-2023-0449.

[6] Vassilatis DK, Hohmann JG, Zeng H, Li F, Ranchalis JE, Mortrud MT, et al. The G protein-coupled receptor repertoires of human and mouse. Proc Natl Acad Sci USA. 2003;100(8):4903–8. doi: 10.1073/pnas.0230374100.

[7] Ketchesin KD, Stinnett GS, Seasholtz AF. Corticotropin-releasing hormone-binding protein and stress: from invertebrates to humans. Stress. 2017;20(5):449–64. doi: 10.1080/10253890.2017.

[8] Bothwell MG. Protein coupled receptors. In: Asbury C, Rieke F, Hille B, Bothwell M, Tuthill J, editors. Physiology. USA: University of Washington; 2023. p. 60–74.

[9] Kuhn CK, Stenzel U, Berndt S, Liebscher I, Schöneberg T, Horn S. The repertoire and structure of adhesion GPCR transcript variants assembled from publicly available deep-sequenced human samples. Nucleic Acids Res. 2024;52(7):3823–36. doi: 10.1093/nar/gkae145.

[10] Zhang Y, Devries ME, Skolnick J. Structure modeling of all identified G protein-coupled receptors in the human genome. PLoS Comput Biol. 2006;2(3):e13. doi: 10.1371/journal.pcbi.0020013.

[11] Bakir B, Sezerman OU. Functional classification of G-protein coupled receptors, based on their specific ligand coupling patterns. In: Rothlauf F, Branke J, Cagnoni S, Costa E, Cotta C, Drechsler R, et al. Applications of evolutionary computing. EvoWorkshops, Lecture notes in computer science. Vol. 3907, Berlin Heidelberg: Springer; 2006. p. 1–12. doi: 10.1007/11732242_1.

[12] Mertens I, Vandingenen A, Meeusen T, De Loof A, Schoofs L. Postgenomic characterization of G-protein-coupled receptors. Pharmacogenomics. 2004;5(6):657–72. doi: 10.1517/14622416.5.6.657.

[13] Kobilka BK. G protein coupled receptor structure and activation. Biochim Biophys Acta. 2007;1768(4):794–807. doi: 10.1016/j.bbamem.2006.10.021.

[14] Zhang D, Zhao Q, Wu B. Structural studies of G protein-coupled receptors. Mol Cell. 2015;38(10):836–42. doi: 10.14348/molcells.2015.0263.

[15] Alhosaini K, Azhar A, Alonazi A, Al-Zoghaibi F. GPCRs: The most promiscuous druggable receptor of the mankind. Saudi Pharm J. 2021;29(6):539–51. doi: 10.1016/j.jsps.2021.04.015.

[16] Hemley CF, McCluskey A, Keller PA. Corticotropin releasing hormone–a GPCR drug target. Curr Drug Targets. 2007;8(1):105–15. doi: 10.2174/138945007779315542.

[17] Majzoub JA. Corticotropin-releasing hormone physiology. Eur J Endocrinol. 2006;155(1):S71–6. doi: 10.1530/eje.1.02247.

[18] Seasholtz AF, Valverde RA, Denver RJ. Corticotropin-releasing hormone-binding protein: biochemistry and function from fishes to mammals. J Endocrinol. 2002;175(1):89–97. doi: 10.1677/joe.0.1750089.

[19] Contoreggi C. Corticotropin releasing hormone and imaging, rethinking the stress axis. Nucl Med Biol. 2015;42(4):323–39. doi: 10.1016/j.nucmedbio.2014.11.008.

[20] Zoumakis E, Makrigiannakis A, Margioris A, Stournaras C, Gravanis A. Corticotropin releasing hormone (CRH) in normal and pregnant uterus: physiological implications. Front Biosci. 1996;1:e1–8. doi: 10.2741/a137.

[21] Kalantaridou SN, Zoumakis E, Makrigiannakis A, Lavasidis LG, Vrekoussis T, Chrousos GP. Corticotropin-releasing hormone, stress and human reproduction: An update. J Reprod Immunol. 2010;85(1):33–9. doi: 10.1016/j.jri.2010.02.005.

[22] Dautzenberg FM, Kilpatrick GJ, Wille S, Hauger RL. The ligand-selective domains of corticotropin-releasing factor type 1 and type 2 receptor reside in different extracellular domains: generation of chimeric receptors with a novel ligand-selective profile. J Neurochem. 1999;73(2):821–9. doi: 10.1046/j.1471-4159.1999.0730821.x.

[23] Kageyama K, Iwasaki Y, Daimon M. Hypothalamic regulation of corticotropin-releasing factor under stress and stress resilience. Int J Mol Sci. 2021;22(22):12242. doi: 10.3390/ijms222212242.
[24] Zouboulis CC, Seltmann H, Hiroi N, Chen W, Young M, Oeff M, et al. Corticotropin-releasing hormone: an autocrine hormone that promotes lipogenesis in human sebocytes. Proc Natl Acad Sci USA. 2002;99(10):7148–53. doi: 10.1073/pnas.102180999.
[25] Trainer PJ, Woods RJ, Korbonits M, Popovic V, Stewart PM, Lowry PJ, et al. The pathophysiology of circulating corticotropin-releasing hormone-binding protein levels in the human. J Clin Endocrinol Metab. 1998;83(5):1611–4. doi: 10.1210/jcem.83.5.4751.
[26] Zhang Y. I-TASSER: fully automated protein structure prediction in CASP8. Proteins. 2009;77:100–13. doi: 10.1002/prot.22588.
[27] Rashid Ur H, Bolzani V, Khan K, Dutra LA, Ahmad N, Wadood A. Homology modeling of alpha-glucosidase from Candida albicans: Sequence analysis and structural validation studies in silico. J Braz Chem Soc. 2024;35(3):e-20230123. doi: 10.21577/0103-5053.20230123.
[28] Find your protein. http://www.uniprot.org, accessed in January 2024.
[29] About GPCR-I-TASSER server. https://zhanggroup.org/GPCR-I-TASSER/about.html. accessed in January 2024.
[30] Basha SH, Talluri D, Raminni NP. Computational repositioning of ethno medicine elucidated gB-gH-gL complex as novel anti herpes drug target. BMC Complement Altern Med. 2013;13:85. doi: 10.1186/1472-6882-13-85.
[31] Molecular Operating Environment (MOE), 2011. 10; Chemical Computing Group Inc., Montreal, QC, Canada, 2012.
[32] Zheng W, Wuyun Q, Zhou X, Li Y, Freddolino P, Zhang Y. LOMETS3: Integrating deep-learning and profile-alignment for advanced protein template recognition and function annotation. Nucleic Acids Res. 2022;50(W1):W454–64. doi: 10.1093/nar/gkac248.
[33] Shi J, Blundell TL, Mizuguchi K. FUGUE: Sequence-structure homology recognition using environment-specific substitution tables and structure-dependent gap penalties. J Mol Biol. 2001;310(1):243–57. doi: 10.1006/jmbi.2001.4762.
[34] Steinegger M, Meier M, Mirdita M, Vöhringer H, Haunsberger SJ, Söding J. HH-suite3 for fast remote homology detection and deep protein annotation. BMC Bioinf. 2019;20(1):473. doi: 10.1186/s12859-019-3019-7.
[35] Wu S, Zhang Y. MUSTER: Improving protein sequence profile-profile alignments by using multiple sources of structure information. Proteins. 2008;72(2):547–56. doi: 10.1002/prot.21945.
[36] Kim D, Xu D, Guo JT, Ellrott K, Xu Y. PROSPECT II: Protein structure prediction program for genome-scale applications. Protein Eng. 2003;16(9):641–50. doi: 10.1093/protein/gzg081.
[37] von Ohsen N, Sommer I, Zimmer R. Profile-profile alignment: A powerful tool for protein structure prediction. Pac Symp Biocomput. 2003;8:252–63.
[38] Zhou H, Zhou Y. Fold recognition by combining sequence profiles derived from evolution and from depth-dependent structural alignment of fragments. Proteins. 2005;58(2):321–8. doi: 10.1002/prot.20308.
[39] Zhou H, Zhou Y. Single-body residue-level knowledge-based energy score combined with sequence-profile and secondary structure information for fold recognition. Proteins. 2004;55(4):1005–13. doi: 10.1002/prot.20007.
[40] Huang SY, Zou X. Advances and challenges in protein-ligand docking. Int J Mol Sci. 2010 Aug;11(8):3016–34. doi: 10.3390/ijms11083016.
[41] Agu PC, Afiukwa CA, Orji OU, Ezeh EM, Ofoke IH, Ogbu CO, et al. Molecular docking as a tool for the discovery of molecular targets of nutraceuticals in diseases management. Sci Rep. 2023;13(1):13398. doi: 10.1038/s41598-023-40160-2.
[42] Ramachandran GN, Ramakrishnan C, Sasisekharan V. RAMPAGE (CCP4: Supported Program), rampage Ramachandran plots using the Richardsons' data. San Francisco, California, United States: Linux Foundation; 1963.
[43] Ramachandran GN, Ramakrishnan C, Sasisekharan V. Stereochemistry of polypeptide chain configurations. J Mol Biol. 1963;7:95–9. doi: 10.1016/s0022-2836(63)80023-6.
[44] Colovos C, Yeates TO. ERRAT: An empirical atom-based method for validating protein structures, online server. USA: National Health Institute, University of California; 1993–2015.
[45] Colovos C, Yeates TO. Verification of protein structures: patterns of nonbonded atomic interactions. Protein Sci. 1993;2(9):1511–9. doi: 10.1002/pro.5560020916.